^{1}H, ^{13}C, ^{15}N resonance assignment of the chitin-active lytic polysaccharide monooxygenase *Bl*LPMO10A from *Bacillus licheniformis*

Gaston Courtade[a], Simone Balzer[c], Zarah Forsberg[b], Gustav Vaaje-Kolstad[b], Vincent G. H. Eijsink[b], Finn L. Aachmann[a †]

[a] Department of Biotechnology, Norwegian University of Science and Technology, Sem Sælands vei 6/8, 7491 Trondheim, Norway
[b] Department of Chemistry, Biotechnology and Food Science, Norwegian University of Life Sciences, P.O. Box 5004, 1432 Ås, Norway
[c] Department of Molecular Biology, SINTEF Materials and Chemistry, Sem Sælands vei 2A, 7465, Trondheim, Norway

[†] Correspondence should be addressed: Finn L. Aachmann, Department of Biotechnology, Norwegian University of Science and Technology, Sem Sælands vei 6/8, 7491 Trondheim, Norway. E-mail: finn.l.aachmann@ntnu.no

Abstract
The chitin-active 19.2 kDa lytic polysaccharide monooxygenase *Bl*LPMO10A from *Bacillus licheniformis* has been isotopically labeled and recombinantly expressed. In this paper, we report the ^{1}H, ^{13}C, ^{15}N resonance assignment of *Bl*LPMO10A.

Keywords: lytic polysaccharide monooxygenase (LPMO), AA10, chitin, cellulose

Biological context
Cellulose and chitin are linear insoluble polymers composed of β-(1,4)-linked D-glucose and *N*-acetylglucosamine, respectively. These polysaccharides form crystalline structures, which makes them resistant to enzymatic hydrolysis and poses an obstacle for efficient biomass conversion. In recent years, a new family of copper-dependent redox enzymes with the ability to increase the rate of enzymatic degradation of these recalcitrant polysaccharides has been identified. (Vaaje-Kolstad et al. 2005a; Moser et al. 2008; Harris et al. 2010; Vaaje-Kolstad et al. 2010; Forsberg et al. 2011; Quinlan et al. 2011; Horn et al. 2012). These enzymes, which are abundantly present in biomass-degrading microbes, are today collectively referred to as lytic polysaccharide monooxygenases (LPMOs). In the CAZy database, they are classified as auxiliary activity (AA) families 9 (AA9, formerly GH61), 10 (AA10, formerly CBM33) and 11 (AA11) (see www.cazy.org and (Levasseur et al. 2013)). LPMOs have been shown to catalyze the cleavage of glycosidic bonds in chitin and cellulose through hydroxylation of either carbon within the scissile bond (Vaaje-Kolstad et al. 2010; Quinlan et al., 2011; Phillips et al., 2011; Kim et al., 2014).

Whereas the structures of several LPMOs have been solved by X-ray crystallography (Vaaje-Kolstad et al. 2005b; Karkehabadi et al. 2008; Harris et al. 2010; Quinlan et al. 2011; Vaaje-Kolstad et al. 2012; Li et al. 2012; Hemsworth et al. 2013b; Wu et al. 2013; Hemsworth et al. 2014), the structure of the chitin-active AA10-type LPMO CBP21 from *Serratia marcescens* (PDB ID: 2LHS; correct name *Sm*LPMO10A) is the only one that has been solved by NMR spectroscopy (Aachmann et al. 2012). The core LPMO structure has been described as a compact β-sandwich with a flat surface that includes the protein N-terminus and binds chitin or cellulose through a combination of polar and hydrophobic interactions (Vaaje-Kolstad et al. 2005a; Aachmann et al. 2012; Hemsworth et al. 2013a). The (putative) substrate-binding surfaces of LPMOs in all three families show considerable variation, but contain a conserved catalytic center with a copper-binding site composed of two histidines that bind the metal ion in a histidine brace (Vaaje-Kolstad et al. 2010; Quinlan et al. 2011; Hemsworth et al. 2013b; Hemsworth et al. 2013a). The metal binding site has high affinity for copper(II) and copper(I), and binding of copper has been shown to increase protein stability (Aachmann et al. 2012; Hemsworth et al. 2013b).

The discovery of LPMOs has fundamentally changed our understanding of the degradation of recalcitrant polysaccharides and has opened up novel opportunities for development of cheaper and more efficient enzymatic tools for biomass conversion. So far, little is known about the structural determinants of their varying activities and substrate specificities (e.g. Hemsworth et al., 2013a; Forsberg et al., 2014). It is thus of major importance to investigate the structure and function of LPMOs for both biotechnological and scientific purposes. The NMR assignment data presented here for a chitin-active 19.2 kDa LPMO from *Bacillus licheniformis* (*Bl*LPMO10A) will allow future structural and functional studies of this LPMO.

Methods and experiments
The NMR assignment was performed on recombinantly expressed full length *Bl*LPMO10A (UniProt accession number Q62YN7). The primary gene product carries a native N-terminal leader sequence (residues 1-31), which is cleaved off during translocation to the periplasmic space of *E. coli* resulting in correctly processed *Bl*LPMO10A (residues 32-203).

Cloning was performed in *E. coli* DH5α (Bethesda Research Laboratories). Cells were grown in LB (10 g/L tryptone, 5 g/L yeast extract and 5 g/L NaCl) or LB agar (LB with 15 g/L agar). Growth media were supplemented with 200 μg/mL ampicillin (Sigma-Aldrich) if required. Standard DNA manipulations were performed as described elsewhere (Berg et al. 2009).

The *Bl*LPMO10A coding region was excised from pRSET_B_*Bl*AA10A (cloned by Forsberg et al. 2014) using NdeI and HindIII. In parallel, pGM29ompA (Sletta et al. 2007) was cut with NdeI and partially digested with HindIII to remove the GM-CSF gene. The *BlLPMO10A* insert and the pGM29ompA backbone were ligated to each other resulting in plasmid pJB-oriLP-*Bl*LPMO10A. Correctness of the resulting construct was confirmed by restriction digestion and sequencing of the insert. The final plasmid was transferred to *E. coli* RV308 (ATCC 31608).

A pre-culture was made by inoculating LB containing 200 μg/mL ampicillin with *E. coli* RV308 cells containing the pJB-oriLP-*Bl*LPMO10A plasmid, followed by incubation at 37°C and 225 rpm, overnight. To uniformly label *Bl*LPMO10A with ^{13}C/^{15}N, 500 mL M9 minimal medium was prepared containing 99% (^{15}NH$_4$)$_2$SO$_4$, 98% ^{13}C$_6$-D-glucose, 10 mL Bioexpress Cell Growth Media (Cambridge Isotope Laboratories, Tewksbury, MA, USA) and 200 μg/mL ampicillin. The main culture was made by inoculating M9 minimal medium or 500 mL LB containing 200 μg/mL ampicillin with 1% pre-culture and incubating at 37°C and 225 rpm until OD$_{600}$ ∼ 0.6-0.8 was reached. After cooling the culture on ice for 5 minutes, protein expression was induced with *m*-toluic acid to a final concentration of 100 μM, followed by incubation at 16°C, 225 rpm, overnight. The culture was harvested by centrifugation at 5,500 xg for 6 minutes at 4°C and the supernatant was removed. The cell pellet was re-suspended in 30 mL ice-cold spheroplast buffer (50 mL 1 M Tris-HCl pH 8.5, 85.5 g sucrose and 500 μL of a stock solution of 0.5 M EDTA pH 8.0) with half a tablet of Complete Protease Inhibitor (Roche) and incubated for 5 minutes on ice. The suspension was centrifuged at 6,150 xg at 4°C for 10 minutes and the supernatant was removed. The pellet was incubated at room temperature for 10 minutes, followed by re-suspension in 25 mL ice-cold MilliQ water with half a tablet Complete Protease Inhibitor (Roche). After 45 seconds, 1.25 mL 20 mM MgCl2 was added. The suspension was centrifuged at 15,000 xg at 4°C for 10 minutes and the supernatant was filtered through a 0.22 μm filter.

An ÄKTA FPLC instrument equipped with a weak anion exchange column (5 mL HiTrap DEAE FF, GE Healthcare Life Sciences) was used to purify the protein. The column was prepared by washing with 5 column volumes of 50 mM Tris-HCl (pH 8.5; running buffer). The periplasmic extract was loaded onto the column and unbound protein was washed of the column by passing through 10 column volumes of running buffer. Protein was then eluted using a linear salt gradient from 100% running buffer to 50% elution buffer (50 mM Tris-HCl, pH 8.5, containing 1 M NaCl) over 200 minutes. The flow rate was 4.5 mL/min throughout the experiment. Fractions containing pure *Bl*LPMO10A (assessed by SDS-PAGE) were concentrated using a VivaSpin 20 protein concentrator (10 kDa cut-off, Sartorius). Four samples were made. In two samples, one non-labeled and one ^{13}C, ^{15}N-labeled, the elution buffer was changed to an NMR buffer (25 mM sodium phosphate pH 5.0 and 10 mM NaCl) with D$_2$O added to a final ratio of 90% H$_2$O/10% D$_2$O (Cambridge Isotope Laboratories, Tewksbury, MA, USA). In the two other samples, one non-labeled and one ^{13}C, ^{15}N-labeled, the elution buffer was changed to an NMR buffer (25 mM sodium phosphate pH* 5.0 and 10 mM NaCl) in 99.9% D$_2$O. The final samples contained 1-1.5 mM *Bl*LPMO10A.

The NMR spectra were recorded at 298 K on a Bruker Avance 600 MHz spectrometer equipped with a 5-mm Z-gradient CP-TCI (H/C/N) cryoprobe at the NT-NMR-Center (NMR-Center at the Faculty of Natural Sciences and Technology at the Norwegian University of Science and Technology, Trondheim, Norway). ^{1}H and ^{13}C chemical shifts were referenced internally to the sodium salt of 3-(trimethylsilyl)propanoic acid (TSP), while ^{15}N chemical shifts were referenced indirectly to TSP, based on the absolute frequency ratios (Zhang et al. 2003). Sequence-specific backbone and side-chain assignments of BlLPMO10A were accomplished using ^{15}N-HSQC, ^{13}C-HSQC HNCO, HN(CA)CO, HNCA, HN(CO)CA, CBCANH, CBCA(CO)NH, HBHANH, HBHA(CO)NH, HC(C)H-TOCSY and HC(C)H-COSY spectra. Assignment of the aromatic side-chains was obtained from IP-COSY, TOCSY, NOESY and ^{13}C-HSQC experiments. The NMR data were recorded and processed with Bruker TopSpin version 2.1/3.0 and spectral analysis was performed using CARA version 1.5.1/1.8.4 (Keller 2004).

Assignment and data deposition
We report here the assignment of backbone and side-chain resonances for BlLPMO10A. The ^{15}N-HSQC spectrum of BlLPMO10A, together with the assignment of the resonances is shown in Fig. 1. The backbone and the side-chain assignments are essentially complete (H^N, H$^\alpha$, N, C$^\alpha$, C' > 97%; H and C side-chains > 90%). The amide group (H^N, N) of His1 could not be found, although other nuclei were assigned. None of the exchangeable side-chain protons of Arg and Lys residues were identified. Side-chain amide groups of most Asn and Gln residues were assigned. Most of the protons and some of the carbon atoms of aromatic side-chains were assigned. The chemical shift data have been deposited in the BioMagResBank under the accession number 19984.

Conflict of interest The authors declare that they have no conflict of interest.

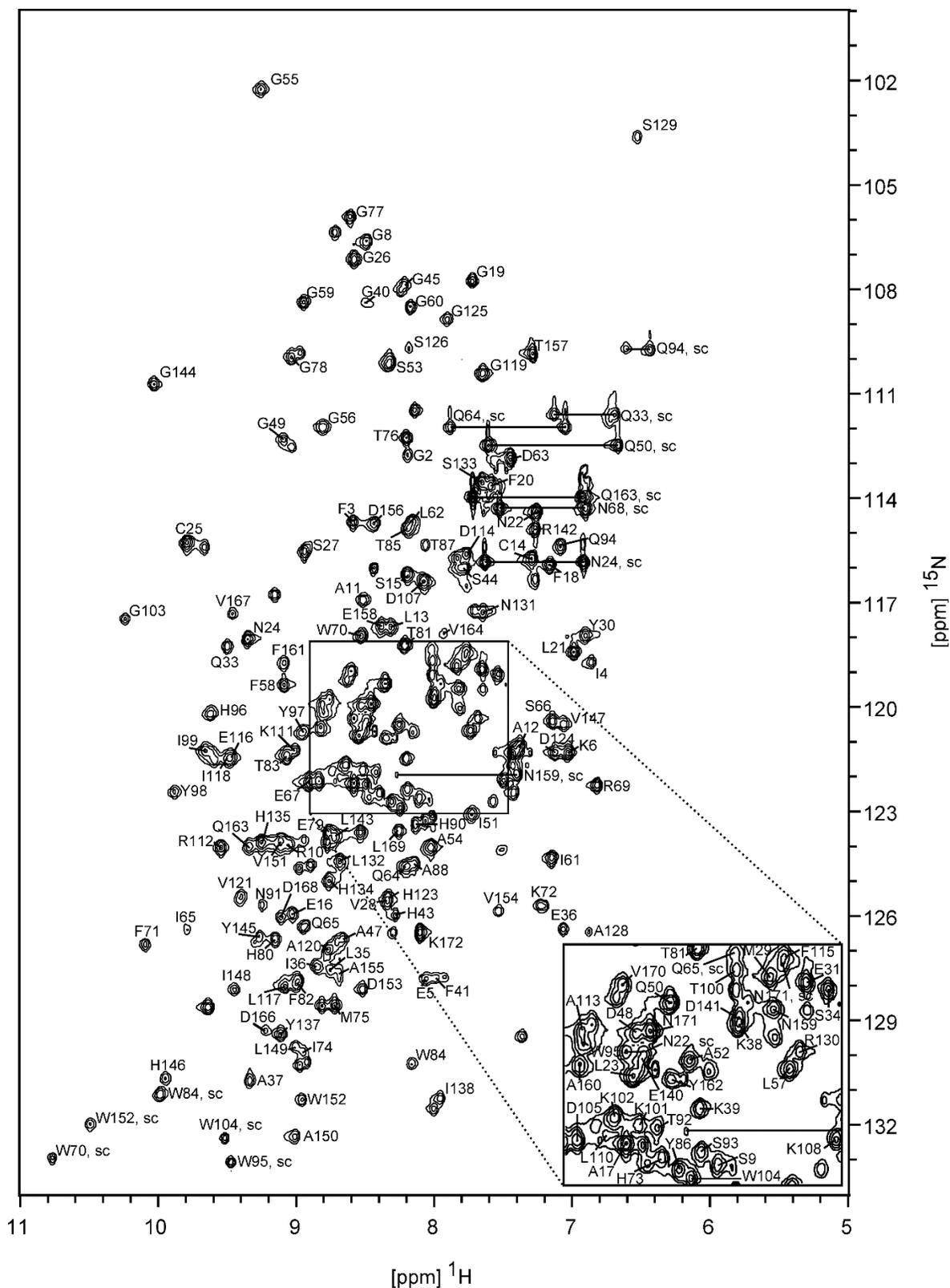**Fig. 1** ^{1}H, ^{15}N HSQC spectrum of ^{13}C, ^{15}N-labeled *Bl*LPMO10A (1.5 mM) from *Bacillus licheniformis* in (90:10) H$_2$O:D$_2$O at pH 5.0, 298 K. Residue types and numbers are indicated. Side-chain resonances of Asn and Gln residues are connected by lines. Other side-chain resonances are indicated with the amino acid number and "sc"

References

Aachmann FL, Sørlie M, Skjåk-Bræk G, et al. (2012) NMR structure of a lytic polysaccharide monooxygenase provides insight into copper binding, protein dynamics, and substrate interactions. Proc Natl Acad Sci U S A 109:18779–18784. doi: 10.1073/pnas.1208822109

Berg L, Lale R, Bakke I, et al. (2009) The expression of recombinant genes in Escherichia coli can be strongly stimulated at the transcript production level by mutating the DNA-region corresponding to the 5'-untranslated part of mRNA. Microb Biotechnol 2:379–389. doi: 10.1111/j.1751-7915.2009.00107.x

Forsberg Z, Røhr AK, Mekasha S, et al. (2014) Comparative Study of Two Chitin-Active and Two Cellulose-Active AA10-Type Lytic Polysaccharide Monooxygenases. Biochemistry 53:1647–1656. doi: 10.1021/bi5000433

Forsberg Z, Vaaje-Kolstad G, Westereng B, et al. (2011) Cleavage of cellulose by a CBM33 protein. Protein Sci 20:1479–1483. doi: 10.1002/pro.689

Harris P V, Welner D, McFarland KC, et al. (2010) Stimulation of lignocellulosic biomass hydrolysis by proteins of glycoside hydrolase family 61: structure and function of a large, enigmatic family. Biochemistry 49:3305–3316. doi: 10.1021/bi100009p

Hemsworth GR, Davies GJ, Walton PH (2013a) Recent insights into copper-containing lytic polysaccharide mono-oxygenases. Curr Opin Struct Biol 23:660–668. doi: 10.1016/j.sbi.2013.05.006

Hemsworth GR, Henrissat B, Davies GJ, Walton PH (2014) Discovery and characterization of a new family of lytic polysaccharide monooxygenases. Nat Chem Biol 10:122–6. doi: 10.1038/nchembio.1417

Hemsworth GR, Taylor EJ, Kim RQ, et al. (2013b) The Copper Active Site of CBM33 Polysaccharide Oxygenases. J Am Chem Soc 135:6069–77. doi: 10.1021/ja402106e

Horn SJ, Vaaje-Kolstad G, Westereng B, Eijsink VG (2012) Novel enzymes for the degradation of cellulose. Biotechnol Biofuels 5:45. doi: 10.1186/1754-6834-5-45

Karkehabadi S, Hansson H, Kim S, et al. (2008) The first structure of a glycoside hydrolase family 61 member, Cel61B from Hypocrea jecorina, at 1.6 Å resolution. J Mol Biol 383:144–154. doi: 10.1016/j.jmb.2008.08.016

Keller R (2004) The Computer Aided Resonance Assignment Tutorial, 1st edn. CANTINA Verlag, Goldau

Levasseur A, Drula E, Lombard V, et al. (2013) Expansion of the enzymatic repertoire of the CAZy database to integrate auxiliary redox enzymes. Biotechnol Biofuels 6:41. doi: 10.1186/1754-6834-6-41

Li X, Beeson WT, Phillips CM, et al. (2012) Structural basis for substrate targeting and catalysis by fungal polysaccharide monooxygenases. Structure 20:1051–1061. doi: 10.1016/j.str.2012.04.002

Moser F, Irwin D, Chen S, Wilson DB (2008) Regulation and characterization of Thermobifida fusca carbohydrate-binding module proteins E7 and E8. Biotechnol Bioeng 100:1066–1077. doi: 10.1002/bit.21856

Quinlan RJ, Sweeney MD, Lo Leggio L, et al. (2011) Insights into the oxidative degradation of cellulose by a copper metalloenzyme that exploits biomass components. Proc Natl Acad Sci U S A 108:15079–15084. doi: 10.1073/pnas.1105776108

Sletta H, Tøndervik A, Hakvåg S, et al. (2007) The presence of N-terminal secretion signal sequences leads to strong stimulation of the total expression levels of three tested medically important proteins during high-cell-density cultivations of Escherichia coli. Appl Environ Microbiol 73:906–912. doi: 10.1128/AEM.01804-06

Vaaje-Kolstad G, Bøhle LA, Gåseidnes S, et al. (2012) Characterization of the chitinolytic machinery of Enterococcus faecalis V583 and high-resolution structure of its oxidative CBM33 enzyme. J Mol Biol 416:239–254. doi: 10.1016/j.jmb.2011.12.033

Vaaje-Kolstad G, Horn SJ, van Aalten DMF, et al. (2005a) The non-catalytic chitin-binding protein CBP21 from Serratia marcescens is essential for chitin degradation. J Biol Chem 280:28492–28497. doi: 10.1074/jbc.M504468200

Vaaje-Kolstad G, Houston DR, Riemen AHK, et al. (2005b) Crystal structure and binding properties of the Serratia marcescens chitin-binding protein CBP21. J Biol Chem 280:11313–11319. doi: 10.1074/jbc.M407175200

Vaaje-Kolstad G, Westereng B, Horn SJ, et al. (2010) An oxidative enzyme boosting the enzymatic conversion of recalcitrant polysaccharides. Science (80-) 330:219–222. doi: 10.1126/science.1192231

Wu M, Beckham GT, Larsson AM, et al. (2013) Crystal structure and computational characterization of the lytic polysaccharide monooxygenase GH61D from the Basidiomycota fungus Phanerochaete chrysosporium. J Biol Chem 288:12828–12839. doi: 10.1074/jbc.M113.459396

Zhang H, Neal S, Wishart DS (2003) RefDB: a database of uniformly referenced protein chemical shifts. J Biomol NMR 25:173–195.